

Near-infrared line spectropolarimetry of hot massive stars

René D. Oudmaijer¹, Janet E. Drew², Jorick S. Vink²

¹ School of Physics & Astronomy, EC Stoner Building, University of Leeds, Leeds LS2 9JT, U.K.

² Imperial College of Science, Technology and Medicine, Blackett Laboratory, Prince Consort Road, London, SW7 2BZ, U.K.

received, accepted

ABSTRACT

In order to study the inner parts of the circumstellar material around optically faint, infrared bright objects, we present the first medium-resolution spectropolarimetric data taken in the near-infrared. In this paper we discuss $\text{Pa}\beta$ line data of GL 490, a well-known embedded massive young stellar object, and of MWC 349A and MWC 342, two optically faint stars that are proposed to be in the pre-main sequence phase of evolution. As a check on the method, the classical Be star ζ Tau, known to display line polarization changes at optical wavelengths, was observed as well. Three of our targets show a “line effect” across $\text{Pa}\beta$. For ζ Tau and MWC 349A this line effect is due to depolarisation by a circumstellar electron-scattering disk. In both cases, the position angle of the polarisation is consistent with that of the larger scale disks imaged at other wavelengths, validating infrared spectropolarimetry as a means to detect flattening on small scales. The tentative detection of a rotation in the polarization position angle at $\text{Pa}\beta$ in the embedded massive young stellar object GL 490 suggests the presence of a small scale rotating accretion disk with an inner hole – similar to those recently discovered at optical wavelengths in Herbig Ae and T Tauri stars.

Key words: polarisation – scattering – stars: circumstellar matter – early type – evolution – pre-main sequence

1 INTRODUCTION

Many open questions regarding the formation and evolution of stars require the ability to probe the inner parts of their circumstellar material, where accretion processes occur and stellar outflows find their origin. A powerful tool to address such issues is spectral line polarimetry. The method can utilise the fact that free electrons in ionised material scatter photons and thereby polarise photospheric radiation. In the case of spherical symmetry, all polarisation vectors cancel, and if the envelope is unresolved a net zero polarisation is observed. On the other hand, if the circumstellar geometry is aspherical, such as a disk, a measurable net polarisation can be observed. This aspect of the method exploits the fact that ionised gas also emits recombination lines, which, by virtue of their location within the extended ionised gas undergo less scatterings by electrons, and will thus be less polarised. A “line-effect” is then observed. Electron scattering typically results in polarisation of order 1% (see Poeckert & Marlborough 1976) and occurs at scales of order several stellar radii (e.g. Cassinelli, Nordsieck & Murison, 1987). The method can be used for objects that display emission lines, and immediately provides the answer to the question whether the circumstellar (electron-scattering) material is spherically symmetric when the source itself cannot be resolved in imaging (e.g. Oudmaijer & Drew 1999, Harries et al. 2002, Schulte-Ladbeck et al. 1993). A further advantage of spectropolarimetry is that it provides additional constraints to straightforward spectroscopy, which

is particularly relevant for follow-up modelling (Drew et al. 2004, Harries 2000, Vink, Harries & Drew 2005a).

Given the debate in the massive star formation community about the respective roles of isolated disk accretion versus competitive accretion in dense cluster environments or even mergers of lower mass protostars, it is crucial to add discriminating observational constraints to this discussion. In particular, it has been argued that the absence of accretion disks in massive young stellar objects (YSOs) is reason to question the relevance of the disk accretion scenario (e.g. Wolfire & Cassinelli 1987; see also Norberg & Maeder 2000). Although a positive detection of a disk around a YSO should by no means be seen as proof for disk accretion, a continuing absence of reliable disk signatures may eventually be taken as evidence against it.

We have obtained spectropolarimetric data of the intermediate mass pre-main sequence Herbig Ae/Be stars using the $\text{H}\alpha$ emission line (Oudmaijer & Drew, 1999, Vink et al. 2002). More than half of the Herbig Ae/Be stars show the line-effect, while the position angles of the circumstellar material are consistent with the, larger scale, disks that in some cases have been imaged by other techniques (see the compilation by Vink et al. 2005b). The high proportion of line effect detections in these objects suggests that *all* Herbig Ae/Be stars are surrounded by disks on small scales. This result provides indirect support to the notion that Herbig Ae/Be stars have grown via accretion.

However, more massive stars with even stronger radiation

Table 1. Targets

Name	<i>V</i>	<i>J</i>	t_{exp} (s)	P_{cont} (%)	Θ_{cont} (°)
GL 490	14	10.5	4800	15.59 ± 0.05	130.1 ± 0.3
MWC 349A	13	7.0	800	3.60 ± 0.04	176.6 ± 0.3
ζ Tau	3	3.2	240	1.10 ± 0.005	35.4 ± 0.1
MWC 342	10.6	~ 6	320	0.40 ± 0.03	152.5 ± 2.3

Continuum polarisations are measured in line-free regions in the spectra. The error bars are internal errors, and small due to the large number of pixels that are averaged. The external errors are estimated to be 0.15% and 2°.

pressure have remained elusive. These most massive young stellar objects stay embedded in their parental cloud until after settling on the zero-age main sequence, which prevents the use of optical line polarimetry. It is therefore necessary to go to (near-)infrared wavelengths to study such objects. This has never been done so far, presumably because common-user polarisation optics at near-infrared optimised telescopes are rare. To do such a study, we first need to consider which line to observe, which is no trivial task. One has to take into account the intrinsic strength of the line, the large extinction towards these objects and the contribution of excess emission due to thermally re-radiating dust. At the longer *K*-band wavelengths the sources suffer less from extinction, but the dust excess emission may set an upper limit to the observable line depolarisations. This is because the magnitude of the “line-effect” is determined by the strength of the intrinsic continuum polarisation against which the change across the unpolarized line is contrasted. Any excess emission due to an extended envelope will effectively dilute the stellar continuum polarisation and consequently this requires more sensitive data. As these issues can not be answered easily pending dedicated observations, we decided to conduct a pilot study to observe optically faint objects and, for the first time, apply this method in the near-infrared. We chose to use the Pa β line in the *J*-band, one of the strongest hydrogen recombination and at a wavelength where the observable continuum radiation is more likely to be dominated by the star.

We observed four objects, MWC 349A, MWC 342 and GL 490, and as a check ζ Tau. The first two objects are optically faint and are proposed to be young pre-main sequence stars while GL 490 is a well-known embedded massive young stellar object. ζ Tau is a classical Be star, known to display a line effect at optical wavelengths. It was observed as well to test and prove the concept.

2 OBSERVATIONS & DATA REDUCTION

The observations were taken during the night of the 26th September 1999 using the UKIRT telescope on Mauna Kea, Hawaii. The weather was reasonable, with a seeing of order 1.3 arcsec. The CGS4 spectrograph was used in conjunction with the 150 lines/mm grating and the long camera. The detector was a 256 \times 256 InSb array which has a pixel size projected on the sky of 0.6 arcsec. During the observations, the slitwidth was 4 pixels (2.4 arcsec), and the slit was oriented East-West. A krypton arc-lamp was used for wavelength calibration. This set-up resulted in a wavelength range of 1.256 - 1.31 μm , with pixels of $\sim 2.1 \times 10^{-4} \mu\text{m}$. The final spectra have a spectral resolution of 170 km s⁻¹. The objects do not appear to be extended in our data.

For the linear polarisation observations, the IRPOL2 instrument was employed. This polarimetry module consists of a MgF₂ prism and a half-waveplate. The QU spectra were recorded at various positions of the waveplate, while the objects were nodded up and down the slit to facilitate sky-subtraction. The observing sequence consisted of consecutive observations of source and sky (by nodding over the slit) for every position of the waveplate. Polarised and un-polarised standards were observed throughout the night. A log of the observations is provided in Table 1.

The data were reduced in IRAF, and included flatfielding, sky and bias subtraction, bad pixel masking and extraction of the spectra. The resulting spectra were then imported in the Starlink¹ Time Series and Polarimetry TSP software, in which the Stokes parameters were determined. Further manipulations were done in the Starlink POLMAP package for the polarisation spectra and IRAF for the intensity spectra.

From the two unpolarised standards, HD 10476 and HD 202573, we determined the instrumental polarisation to be 0.165% at an angle of 122.2°. This value was subtracted from the reduced data. The zero-point of the polarisation angle was determined assuming the polarisation standard stars HD 23512 and HD 43384 to have polarisation angles of 29.6° and 170.7° respectively. These values correspond to the *R* band values listed by Hsu & Breger (1982). The corrections were within 1° from each other. The polarisation measured in the standard stars at 1.28 μm is slightly (0.1%) larger than an extrapolation from their optical data using a Serkowski law would suggest. This is a well-documented effect, the polarisation in the near-infrared drops of shallower than in the optical (e.g. the review by Whittet, 1996).

The errors in polarisation per pixel range from $\sim 0.05 - 0.1\%$ for the brighter stars to 0.25% for MWC 342 and MWC 349A and 0.40% for GL 490. For the brightest objects, the error in the polarisation is observed to increase with increasing wavelength. This is most likely due to low level fringing occurring in the optics. The final, external, accuracies are estimated to be of order 0.15% and 2° respectively.

3 RESULTS

Here we discuss the results individually for the objects. We start by describing the results of the classical Be star ζ Tau, and then continue with the massive young stars. In Table 1 the measured polarisations of the objects are presented.

3.1 ζ Tau

Because ζ Tau has a long history of (spectro)polarimetric observations, it is an ideal object to test the diagnostic power of near-infrared spectropolarimetry. Also, ζ Tau is known to have a large-scale disk found through interferometry, consistent with the intrinsic line polarisation at optical wavelengths (Quirrenbach et al. 1997). Our data are presented in Fig. 1, where the Stokes I (intensity) vector is plotted in the bottom panel, and the polarisation percentage and polarisation angle (PA) are displayed in the middle and upper panels respectively. The polarisation across the Pa β line shows a marked drop with respect to the continuum.

The continuum polarisation of 1.1% is slightly lower and the PA is very close to the optical values of Quirrenbach et al. (1997,

¹ <http://star-www.rl.ac.uk/>

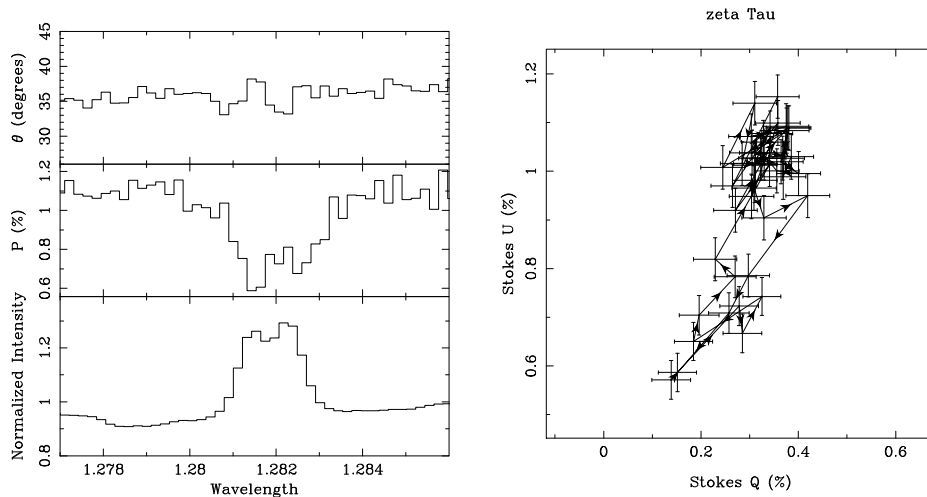


Figure 1. The left hand plot shows the polarisation data of ζ Tau represented as a function of wavelength in μm , the bottom panel shows the (continuum-normalised) intensity spectrum, while the middle and upper panels show the polarisation and position angle respectively. The latter two are rebinned to a corresponding accuracy in the polarisation of 0.05%. The right hand plot shows the Stokes QU vectors with the same binning applied. The excursion of the depolarisation in the QU plane implies a best fitting intrinsic PA of 32° .

their mean values are about 1.5% and 31°). The small change in polarization from the optical to the NIR is not expected from a Serkowski law, where the dust polarisation drops off steeply with wavelength, but is consistent with the flatter dependence from electron scattering. We can measure the *intrinsic* PA from the excursion across the line profile observed in the QU diagram; $\Theta = \frac{1}{2} \times \text{atan}(\Delta U/\Delta Q)$ yielding $32 \pm 1^\circ$. As scattering in the optically thin case gives a PA perpendicular to the disk, this compares very well with the disk’s position angle of $-58 \pm 4^\circ$ measured interferometrically by Quirrenbach et al. (1997).

In summary, the near-infrared spectropolarimetry is a complementary technique to optical spectropolarimetry and interferometry allowing us to move to longer wavelength ranges where we can obtain detailed observational constraints on types of object that would otherwise remain obscured.

3.2 MWC 349A

This well-studied object is mostly considered to be a massive pre-main sequence star (e.g. Danchi, Tuthill & Monnier 2001; Meyer, Nordsieck & Hoffman 2002) although it is sometimes proposed to be an evolved massive star (strong proponents are Hofmann et al. 2002). It had not been previously observed by us at $H\alpha$ as the object is too faint in the optical for medium resolution spectropolarimetry. Our data are plotted in Fig. 2. The $Pa\beta$ line is strongly in emission, whilst the He I 1.27 μm line, blueward of $Pa\beta$, is clearly present as well. The observed continuum polarization of 3.5%, at a PA of $\sim 180^\circ$, is consistent with optical values (Yudin 1996). There is a clear signature of a line effect at $Pa\beta$, particularly seen as a drop in polarization percentage across the line (middle panel).

Representing the data in QU space, such as shown in Fig. 2 allows one to obtain the intrinsic PA of the polarisation *independent* of any foreground polarization, which only adds a constant QU vector to the intrinsic polarization. There is a strong effect over the line, with a magnitude of $\sim 1.5\%$ at a polarization angle of $21 \pm 1^\circ$ as determined from a weighted least squares fit through the QU data points, as above. A similar, less strong effect at the same PA

is visible for the helium line. There is one earlier report of a ‘line-effect’ in MWC 349A: Meyer et al. (2002) obtained low resolution (7.5-10 \AA) optical spectropolarimetry, and reported strong line depolarisations. Earlier, broad-band optical polarimetry accompanied by narrow-band $H\alpha$ polarimetry was obtained by Zickgraf & Schulte-Ladbeck (1989), but they did not report the line-effect, possibly because it was smeared out over the large wavelength range covered by the $H\alpha$ filter.

We also note that although the polarization angle changes by about 10° over the emission line, this does not necessarily have to be an intrinsic property of the polarization. One measures the vector sum of both intrinsic and interstellar polarization. Due to this vectorial nature, a simple depolarisation can change into a more complicated profile with the addition of ISP (see e.g. Oudmaijer et al. 1998 for a marked change in the case of HD 87643). The linear excursion observed in QU space strongly suggests that we deal with a straightforward depolarisation.

The obvious question that now arises is where does the scattering arise, in the well-known ionised North-South bipolar outflow visible in the radio (White & Becker 1985) or the East-West circumstellar disk as is evident from imaging of hydrogen recombination line masers (e.g. Planesas, Martin-Pintado & Serabyn 1992; Rodriguez & Bastian 1994)? As mentioned in the previous subsection, in the optically thin case we will measure a polarization angle perpendicular to the disk plane, while modelling of Be star disks implies polarization percentages not much more than 2% (Cassinelli et al. 1987; Waters & Marlborough 1992), with the polarization decreasing with inclination angle.

The intrinsic position angle of the polarization is $21 \pm 1^\circ$, which is almost perpendicular to the position angle of $107 \pm 7^\circ$, measured from the $H30\alpha$ line maser (Planesas et al. 1992) and the $100 \pm 3^\circ$ measured from interferometric images tracing warm dust (Danchi et al. 2001). This is consistent with the scattering occurring in a structure at the same PA. As the larger scale disk is observed to be close to edge-on, the depolarization of about 1.5% lends extra support to the idea that the spectropolarimetry, and associated line effects, are due to a circumstellar ionized disk.

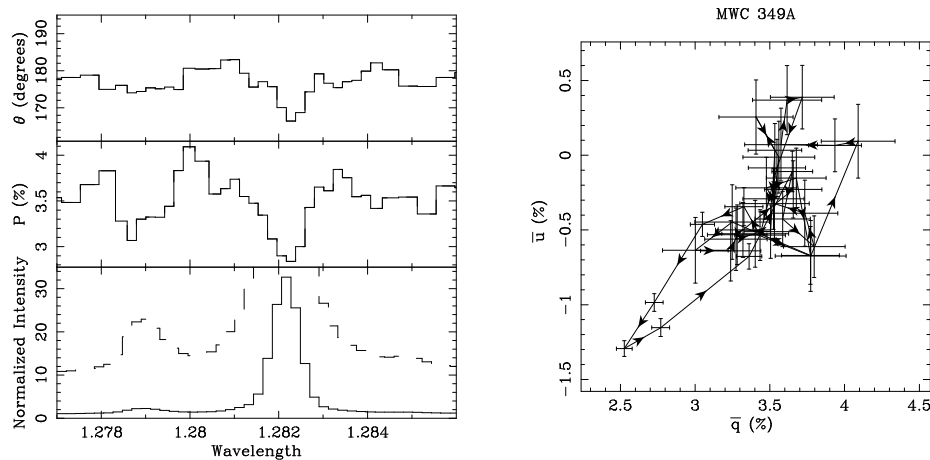


Figure 2. As previous figure. The polarization data of MWC 349A rebinned to 0.25%. The dashed line is an enhanced version of the intensity spectrum intended to reveal the relatively strong, twice the continuum, He I λ 1.27842 μ m line. The polarization spectrum shows an effect across both the Pa β and He I emission lines. The depolarization is smaller across the He I line because of the relatively larger contribution of the continuum to the observed polarization.

Since MWC 349A is such a well-observed object, we now consider how our Pa β data fit in with existing ideas about the ionized gas around this object. Spectropolarimetry should be particularly helpful as it, in principle, probes the ionized gas close to the star.

Hamann & Simon (1986, 1988) proposed a model of the circumstellar material, based on velocity resolved optical and near-infrared spectroscopy of the star. They found that the line-width, and peak separation of resolved hydrogen recombination lines decreased as function of distance to the star. The Helium recombination lines showed the largest widths, and were suggested to be originating at the inner edge of a Keplerian rotating circumstellar disk at a distance of $\simeq 2$ AU from the star. The hydrogen recombination lines, especially optically thick lines like H α , were placed much further from the star, consistent with the observed extent of the hydrogen masers at 60 AU and more (e.g. Planesas et al. 1992). The authors explicitly introduced a low density region between the star and the disk/wind. This is mainly because of the observed line-widths: if MWC 349 is indeed a massive hot star, the line widths of order 100 km s $^{-1}$ are too small to be identified with a hot stellar wind whose observed velocities are generally larger. Instead, Hamann & Simon locate the ionised gas in a photo-evaporating disk (see also Hollenbach et al. 1994), further away from the star, where the local escape velocity is low. This would present a coherent picture, where a comparatively low density fully ionised inner disk is responsible for the observed electron-scattering induced polarization.

We wish to mention a possible alternative that can explain the low outflow velocity and still be consistent with a circumstellar disk. Drew, Proga & Stone (1998) present a hydrodynamical model of radiation driven disk winds for YSOs that also predict narrow HI line emission in the equatorial plane, and higher velocity, more tenuous emission in the polar regions. Such a model could also be responsible for the observed line-profiles in MWC 349A.

3.3 MWC 342

This object, often classed a young Herbig Be star, has a rich emission line spectrum with H α displaying a P Cygni profile, indicating current outflow, while the presence of many forbidden emission lines class the object a B[e] star (Jaschek & Andriolat 1999). The most in-depth study to date of MWC 342 is probably that of Miroshnichenko & Corporon (1999) who suggest the object is a luminous evolved star based on its extinction distance. The literature does not report any observations that specifically study the geometry of the circumstellar material. Clues that at least some asymmetries are present come from the variable optical polarization reported by Bergner et al. (1990). The continuum polarization around Pa β of this object is 0.4%. This makes it the least polarized of the objects in our sample and corresponds to a phase of low optical polarization (Bergner et al 1990, Miroshnichenko, private communication). The data are plotted in Fig. 3 but no line effect can be inferred with confidence. Since the polarization across the line measured per pixel is only at the 2σ level - as opposed to the value derived in Table 1 which is derived from many pixels - it is hard to measure an effect at a significant level, and easy to overinterpret such data. Rebinning the data would yield severely undersampled data and potentially lead to misleading results. The uncertainty in polarization of the individual pixels is 0.25%, so the upper limit to the line-depolarisation is at least 0.75%, as an entire resolution element needs to be covered.

3.4 GL 490

AFGL 490 is a heavily embedded massive young star with a luminosity of order $10^3 L_{\odot}$ (e.g. Schreyer et al. 2002). It is subject to an optical extinction > 20 (Bunn et al. 1995), and is surrounded by a thick dusty disk at a PA of around 120-145 $^{\circ}$. The disk structure has been observed using a variety of techniques: near-infrared imaging was done by Minchin et al. (1991); high resolution molecular CS observations were taken by Schreyer et al. (2002), whilst Alvarez et al. (2004) detect a, possibly transient, structure in near-infrared speckle interferometry. In addition, a flattened radio structure was

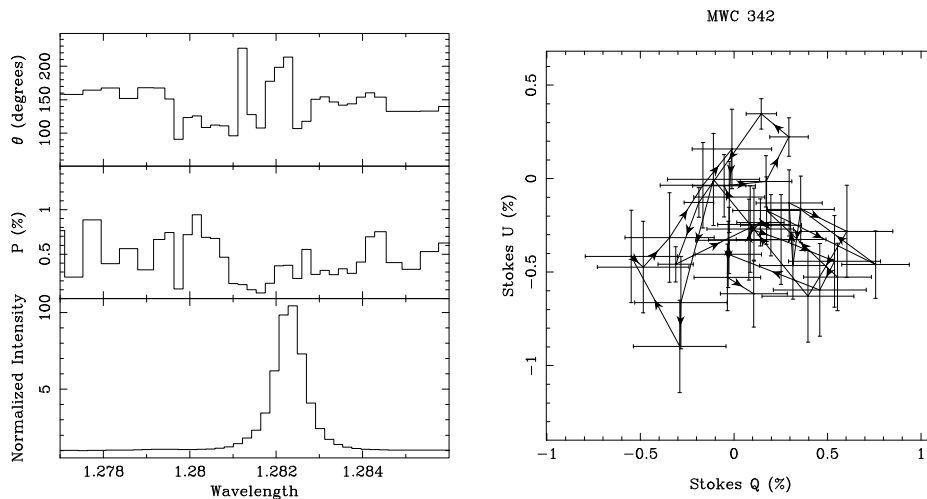


Figure 3. As previous figures, but now the polarization data of MWC 342 rebinned to 0.25% are plotted. The large errorbars combined with the low polarization prevent the detection of a line-effect.

found by Campbell, Persson & McGregor (1986). The central object powers a wide bi-polar CO outflow roughly perpendicular to the disk (e.g. Mitchell et al. 1995, Schreyer et al. 2002).

The optical polarization was studied by Haas, Leinert & Lenzen (1992). They found that the bulk of the optical polarization of $\sim 18\%$ can be explained by a combination of foreground polarization (surrounding stars have optical polarizations of up to 13%) and polarization by circumstellar dust. As electron scattering typically would contribute around 1-2%, it is indeed most likely the dust scattering, rather than electron scattering that contributes most to the circumstellar polarization. Because the dust can not exist close to the star owing to its comparatively low condensation temperature, the Pa β line forming region and the central source continuum will be seen as a point sources by the dust and be equally polarized. Although the observed polarization is a combination of interstellar dust and circumstellar dust and electron-scattering, the “intrinsic” electron scattered radiation is revealed in *QU* space, as the interstellar and circumstellar dust polarization will add respective constant *QU* polarization vectors, whereas the intrinsic electron scattering polarization can be dependent on the velocities.

Our polarimetric spectrum of GL 490 is presented in Fig. 4. The emission line itself is resolved as it is slightly wider than the instrumental profile, thereby allowing the study of changes in the polarization characteristics across the line itself. We measure a continuum polarization of $\sim 15\%$ at a PA of 130° , which is consistent with the PA measured by Haas et al. (1992) in optical continuum polarization measurements, and also with with the large scale dusty disk seen using imaging polarimetry (Minchin et al. 1991). In the polarisation triplot, there appears evidence of changes in line polarisation, in particular a rotation in the PA. This is most likely a real feature because the emission line is resolved in our data while the feature is larger than the formal errorbars in both the PA spectrum, and the *QU* graph.

We note that this effect may well be similar to the line effects measured in many Herbig Ae stars by Vink et al. (2002). In their work on these objects they found that the polarisation changes across H α were narrower than the width of the intensity profile itself – which is inconsistent with depolarisation. Instead, the data showed line polarisations that are thought to be due to H α emission

originating from a compact source of photons that scatters off an exterior rotating medium. In contrast to the effect of depolarisation observed for MWC 349A, these line polarisations may yield kinematic information. The PA rotations across the line profile translate into “loops” when the same data are plotted in *QU* space.

Indeed, the excursion in *QU* space resembles a loop, rather than the straight line observed for MWC 349A. Comparison with models by Vink et al (2005a, see also Wood, Brown & Fox 1993) indicates that such behaviour is the result of the presence of a rotating disk with an inner hole. For comparison, rotating disks without an inner hole, extending down to the stellar photosphere would display a double loop in the *QU* diagram. If the detection is can be confirmed, it provides strong clues that GL 490 is surrounded by a disk and is still actively accreting material.

4 SUMMARY

We have presented the first hydrogen recombination line spectropolarimetric observations in the near-infrared. The results from this study are encouraging. Our targets were two optically bright Herbig Be type objects (MWC 349A and MWC 342), an optically faint massive Young Stellar Object, GL 490 and for comparison the well-known classical Be star ζ Tau, known to be surrounded by an ionised disk.

Three of these stars show a line effect. For ζ Tau and MWC 349A the line-effect is explained as being due to optically-thin electron scattering in a circumstellar disk. These objects have high-resolution imaging data available and in both cases the position angle of the (larger scale) disk on the sky is consistent with the angle derived from the polarization data. This validates spectropolarimetry as a good means to detect disks on small scales.

The preliminary detection of a PA rotation in GL 490 may indicate the presence of a small scale rotating accretion disk with an inner hole similar to those recently discovered in H α in Herbig Ae and T Tauri stars (Vink et al. 2002, 2005b).

Acknowledgements : We thank Tim Harries for discussing the intricacies of reducing near-infrared spectropolarimetric data. We thank Anatoly Miroshnichenko for providing us with machine readable

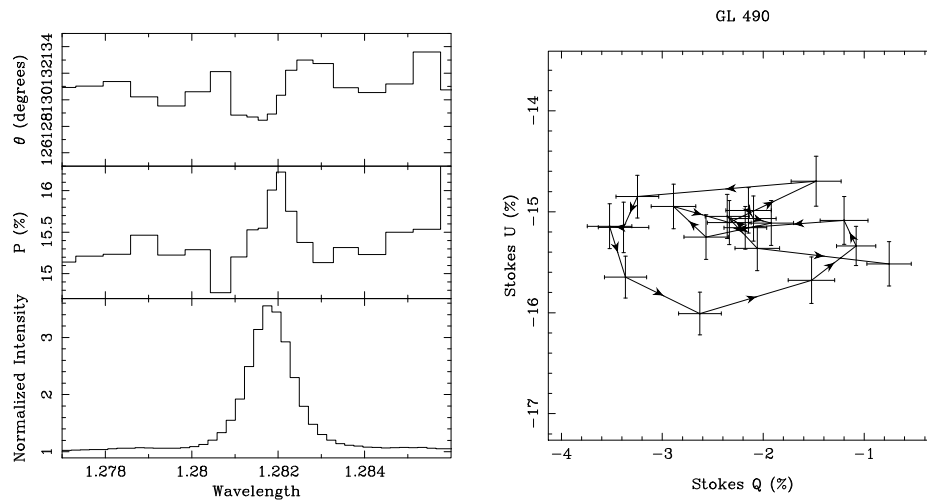


Figure 4. As the previous figures. The polarization data of GL 490, rebinned to 0.25% per pixel.

data from the Bergner et al. (1990) paper, supplemented by additional unpublished polarimetry. The United Kingdom Infrared Telescope is operated by the Joint Astronomy Centre on behalf of the UK Particle Physics and Astronomy Research Council. JSV is funded by PPARC. IRAF is written and supported by the IRAF programming group at the National Optical Astronomy Observatories (NOAO) in Tucson, Arizona. NOAO is operated by the Association of Universities for Research in Astronomy (AURA), Inc. under cooperative agreement with the National Science Foundation

REFERENCES

- Alvarez C., Hoare M.G., Glindemann A., Richichi A. 2004, *A&A* 427, 505
 Bergner Y.K., Miroshnichenko A.S., Sudnik I.S., Yudin R.V., Yutanov N.Y., Krivtsov A.A., Sokolov A.N., Kuratov K.S., Mukanov D.B. 1990, *Afz* 32, 203
 Bunn J.C., Hoare M.G., Drew J.E., 1995, *MNRAS* 272, 346
 Campbell B., Persson S.E., McGregor P.J. 1986, *ApJ* 305
 Cassinelli J.P., Nordsieck K.H., Murison M.A. 1987, *ApJ* 317, 290
 Danchi W.C., Tuthill P.G., Monnier J.D. 2001, *ApJ* 562, 440
 Drew J.E., Proga D., Stone J. M., 1998, *MNRAS* 296, L6
 Drew J.E., Vink J.S., Harries T.J., Kurosawa R., Oudmaijer R.D., 2004, to appear in Proceedings of ESO Conference on high resolution IR spectroscopy, astro-ph/0403672
 Haas M., Leinert Ch., Lenzen R. 1992, *A&A* 261, 130
 Hamann F., Simon M. 1986, *ApJ* 311, 909
 Hamann F., Simon M. 1988, *ApJ* 327, 876
 Harries T.J. 2000, *MNRAS* 315, 722
 Harries T.J., Monnier J.D., Symington N.H., Kurosawa R. 2002, *MNRAS* 337, 341
 Hofmann K.-H., Balega Y., Ikhsanov N.R., Miroshnichenko A., Weigelt G. 2002, *A&A* 395, 891
 Hollenbach D., Johnstone D., Lizano S., Shu F., 1994, *ApJ* 428, 654
 Hsu J.-C., Breger M. 1982, *ApJ* 262, 732
 Jaschek C., Andrillat Y. 1999, *A&AS* 136, 59
 Meyer J.M., Nordsieck K.H., Hoffman J.L. 2002, *AJ* 123, 1639
 Minchin N.R., Hough J.H., Burton M.G., Yamashita T. 1991, *MNRAS* 251, 522
 Miroshnichenko A., Corporon P. 1999, *A&A* 349, 126
 Mitchell G.F., Lee S.W., Maillard J.-P., Matthews H., Hasegawa T.I., Harris A.I. 1995, *ApJ* 438, 794
 Norberg P., Maeder A. 2000, *A&A* 359, 1035
 Oudmaijer R.D., Proga D., Drew J.E., de Winter D. 1998, *MNRAS* 300, 170
 Oudmaijer R.D., Drew J.E. 1999, *MNRAS* 305, 166
 Planesas P., Martin-Pintado J., Serabyn E. 1992, *ApJ* 386, 23
 Poeckert R., Marlborough J.M. 1976, *ApJ* 206, 182
 Quirrenbach A., Bjorkman K.S., Bjorkman J.E. et al., 1997, *ApJ*, 479, 477
 Rodriguez L.F., Bastian T.S. 1994, *ApJ* 428, 324
 Schreyer K., Henning Th., van der Tak F.F.S., Boonman A.M.S., van Dishoeck E.F. 2002, *A&A* 394, 561
 Schulte-Ladbeck R.E., Leitherer C., Clayton G.C., Robert C., Meade M.R., Drissen L., Nota A., Schmutz W. 1993, 407, 723
 Vink J.S., Drew J.E., Harries T.J., Oudmaijer R.D. 2002, *MNRAS* 337, 356
 Vink J.S., Harries T.J., Drew J.E. 2005a *A&A* 430, 213
 Vink J.S., Drew J.E., Harries T.J., Oudmaijer R.D., Unruh Y. 2005b, *MNRAS* 359, 1049
 Waters L.B.F.M., Marlborough J.M., 1992, *A&A* 256, 195
 White R.J., Becker R.H. 1985, *ApJ* 297, 677
 Whittet D.C.B. 1996, in "Polarimetry of the ISM", eds. W.G. Roberge and D.C.B. Whittet, ASP Conf. Series 97, 125
 Wolfire M.G., Cassinelli J.P. 1987, *ApJ* 319, 850
 Wood K., Brown J. C., Fox G.K., 1993, *A&A* 271, 492
 Yudin R.V. 1996, *A&A* 312, 234
 Zickgraf F.-J., Schulte-Ladbeck R.E. 1989, *A&A* 214, 274